Figures and figure supplements

Doublecortin and JIP3 are neural-specific counteracting regulators of dynein-mediated retrograde trafficking

Xiaoqin Fu *et al.*

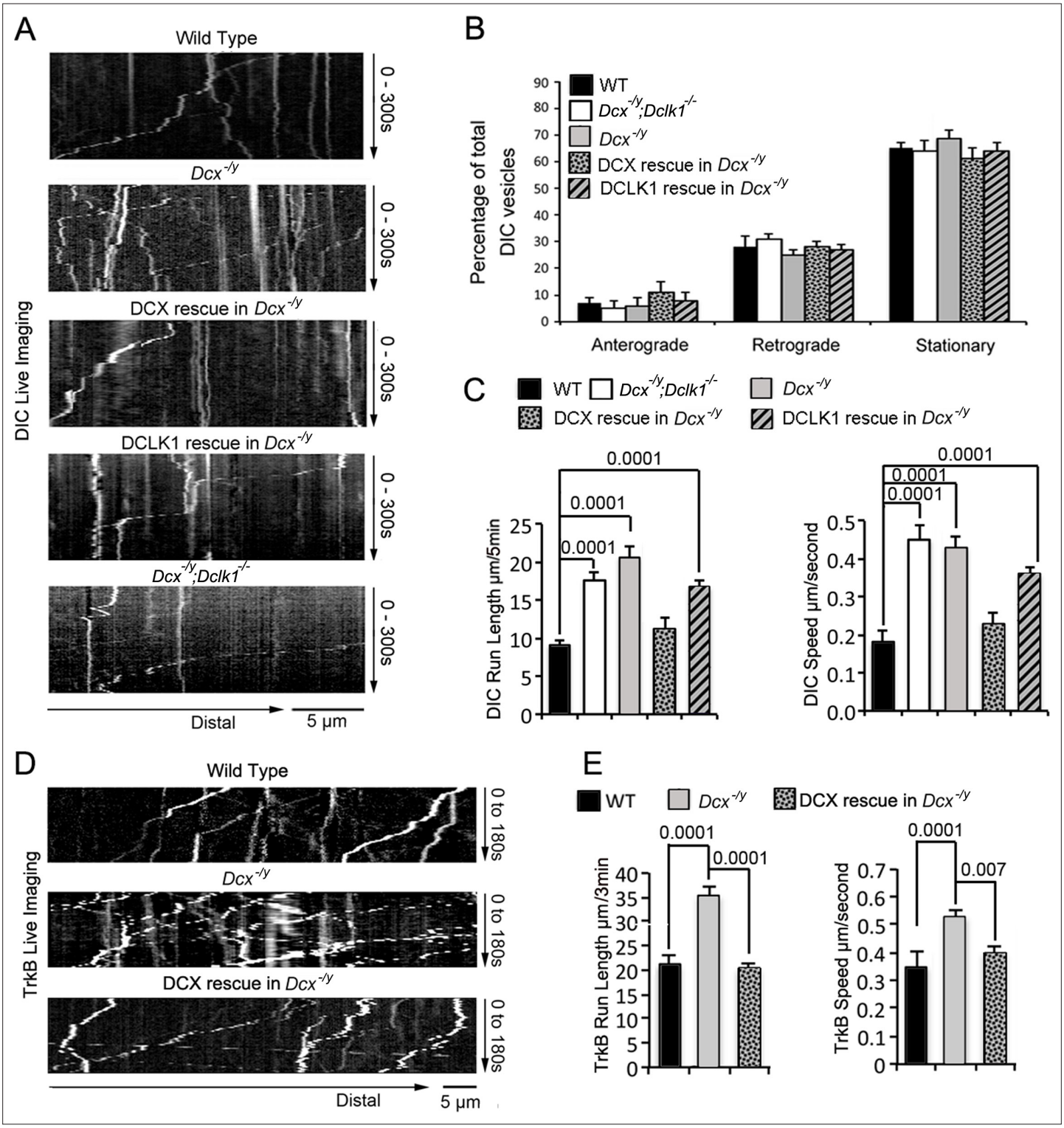

Figure 1. The retrograde trafficking of the dynein motor and TrkB transport is increased in axons without doublecortin (DCX). (**A**) WT, *Dcx*$^{-/y}$ or *Dcx*$^{-/y}$;*Dclk1*$^{-/-}$ associated cortical neuronal culture were transfected with plasmids expressing DIC-RFP on days in vitro (DIV) 6 and imaged on DIV8. For rescue experiments, *Dcx*$^{-/y}$ neurons were transfected with plasmids expressing DIC-RFP combined with plasmids expressing either DCX-GFP or DCLK1-GFP. Representative kymographs of DIC-RFP transport in axons are shown. (**B**) Distribution calculations of the DIC vesicle mobility status (anterograde, retrograde, and stationary) are demonstrated. No significant differences are observed among different neurons. (**C**) Quantifications of DIC-RFP run length (mean+/- SEM) within 300 s and velocity (mean+/-SEM) are shown. DCX, but not DCLK1, fully rescued the increased dynein motor transport observed in DCX-deficient axons. p-Values comparing WT and DCX rescue for run length and speed are 0.57 and 0.18, respectively. Other p-values are

Figure 1 continued on next page

Figure 1 continued

shown in the figure. (**D**) Dissociated cortical neuronal cultures from WT or *Dcx*$^{-/y}$ mice were transfected with plasmids expressing TrkB-RFP with/without plasmids expressing DCX-GFP on DIV6 and imaged on DIV8. Representative kymographs of TrkB-RFP transport in axons are shown. (**E**) Quantification of vesicle run length (mean+/- SEM) within 180 s and velocity (mean+/- SEM) are demonstrated. DCX rescued the increased TrkB-RFP transport in DCX-deficient axons. Data are based on three independent experiments of each condition. Total numbers of neurons (N) and vesicles (V) used in the calculations are indicated in ***Figure 1—figure supplement 1***.

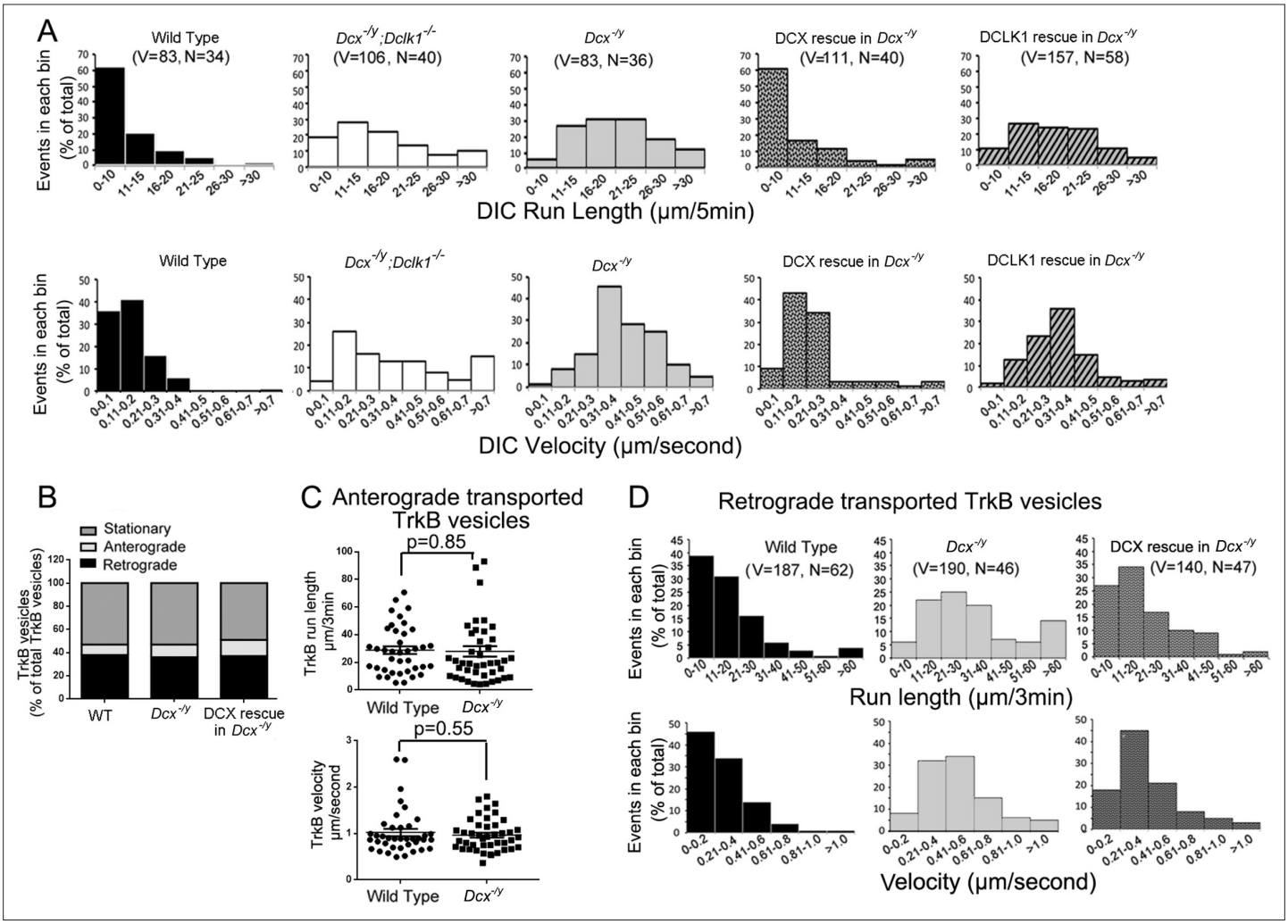

Figure 1—figure supplement 1. Run length and velocity distributions of dynein intermediate chain (DIC) and TrkB in different neurons. (**A**) Run length and velocity distributions of retrograde DIC complexes in different neurons are shown. Total numbers of neurons (N) and vesicles (V) used in the calculations are indicated in the panel. (**B**) Distribution calculations of the TrkB vesicle mobility status (anterograde, retrograde, and stationary) are demonstrated. No significant differences are observed among different neurons from test. (**C**) The analysis of anterograde transport of TrkB vesicles. No significant differences are observed in both velocity and run length of anterogradely transported TrkB vesicles between wild type (39 vesicles from 27 neurons, n = 4) and *Dcx*$^{-/y}$ neurons (43 vesicles from 27 neurons, n = 4). (**D**) Run length and velocity distributions of retrograde TrkB complexes in different neurons are shown. Total numbers of neurons (N) and vesicles (V) used in the calculations are indicated in the panel.

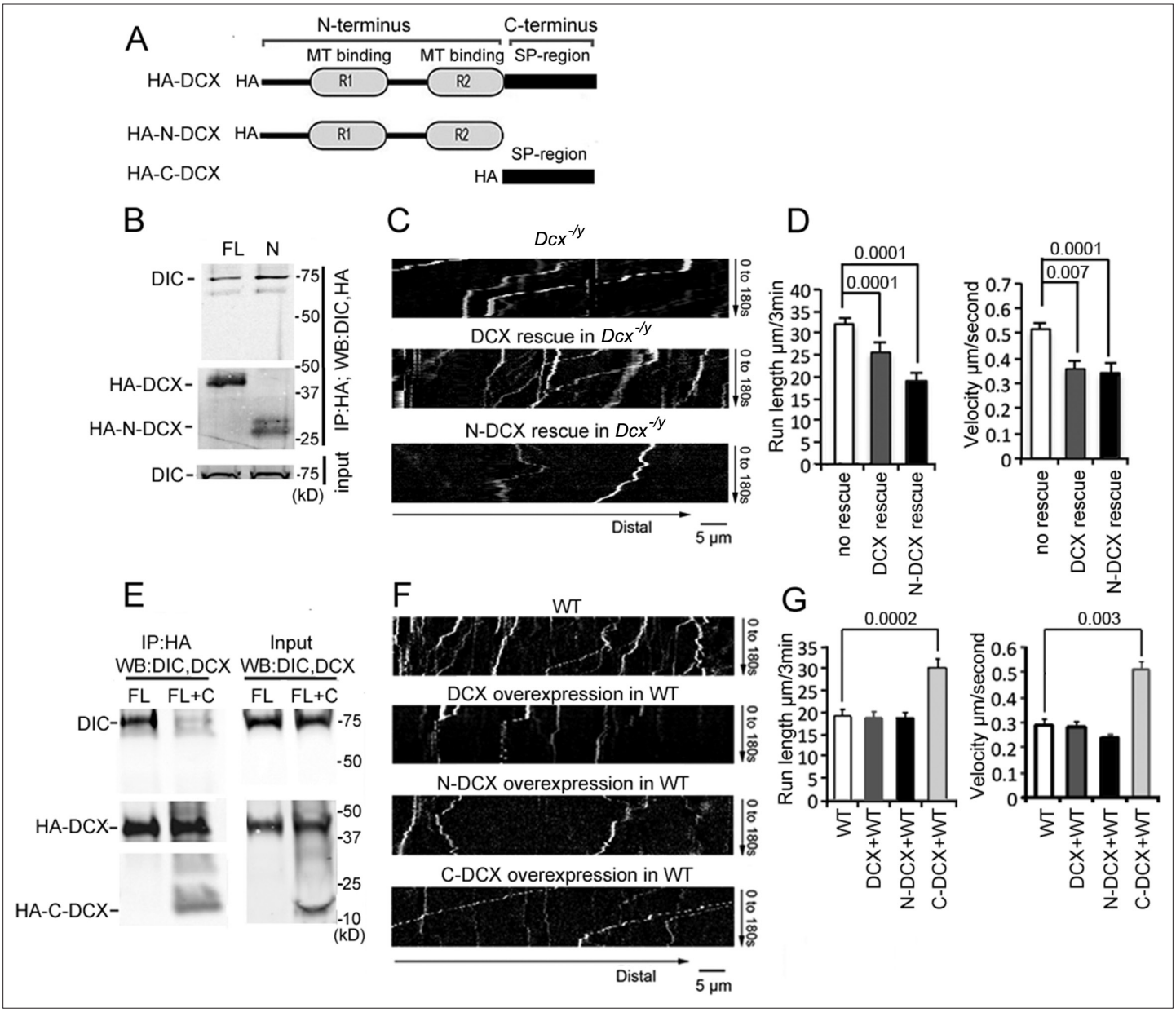

Figure 2. Doublecortin (DCX) affects the retrograde transport through DCX/dynein interaction. (**A**) A schematic of DCX protein domain structure. N-DCX has N-terminal R1 and R2 domains representing microtubule (MT)-binding domains of DCX, while C-DCX has DCX C-terminal serine/proline (SP) rich domain. (**B**) More N-DCX proteins are pulled down with DIC compared with full-length DCX. HEK293 cells were transfected with plasmids expressing HA-tagged either full-length DCX (FL) or N-DCX (N) for 2 days. Protein lysates were used for immunoprecipitation using antibodies for HA and analyzed by Western blot for DIC and HA. (**C**) Dissociated cortical neuronal culture from *Dcx*$^{-/y}$;*Dclk1*$^{-/-}$ mice were transfected with plasmids expressing TrkB-RFP with/without plasmids expressing DCX or N-DCX on days in vitro (DIV)6 and imaged on DIV8. Representative kymographs of TrkB-RFP transports in axons are shown. (**D**) Quantifications of TrkB-RFP run length (mean+/- SEM) within 180s and velocity (mean+/-SEM) are shown. The expression of either full-length DCX or N-DCX in DCX knockout neurons significantly decreased TrkB retrograde transport while N-DCX has stronger effect compared with full-length DCX. (**E**) C-DCX decreases DCX/DIC association. HEK293 cells were transfected with plasmids expressing HA-tagged full-length DCX (FL) with/without plasmid expressing C-DCX for 2 days. Protein lysates were used for immunoprecipitation using antibodies for HA and analyzed by Western blot for DIC and HA. (**F**) Dissociated cortical neuronal culture from wild-type mice were transfected with plasmids expressing TrkB-RFP with/without plasmids expressing DCX, N-DCX, or C-DCX on DIV6 and imaged on DIV8. Representative kymographs of TrkB-RFP transports in axons are shown. (**G**) Run length within 180 s and velocity distributions of retrograde TrkB complexes in axons are quantified. C-DCX overexpression in wild-type neurons mimicked the phenotype of TrkB retrograde trafficking observed in *Dcx*$^{-/y}$ axons. All quantification data are based on three independent experiments of each condition. p-Values from *t*-tests are shown in each panel. Total numbers of neurons (N) and vesicles (V) used in the calculations are indicated in ***Figure 2—figure supplement 2***. See also ***Figure 2—figure supplement 1***.

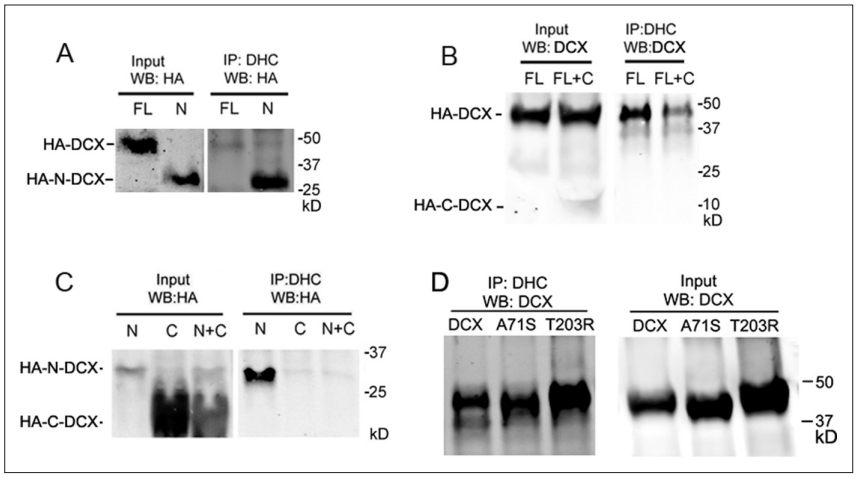

Figure 2—figure supplement 1. Doublecortin (DCX) associates with dynein heavy chain through its N-terminal domain. (**A**) HEK293 cells are transfected with full-length DCX (FL) or N-DCX (N) for 2 days. Protein lysates were used for immunoprecipitation and analyzed by Western blot as indicated in the figure. More N-DCX proteins are precipitated with DHC compared to full-length DCX, while similar amount of full-length DCX and N-DCX is expressed in transfected cells. (**B**) HEK293 cells are transfected with full-length DCX (FL) with/without C-DCX (**C**) for 2 days. The presence of C-DCX decreases association of full-length DCX with DHC. (**C**) Similarly, C-DCX decreases the association of N-DCX with DHC. C-DCX does not bind DHC.

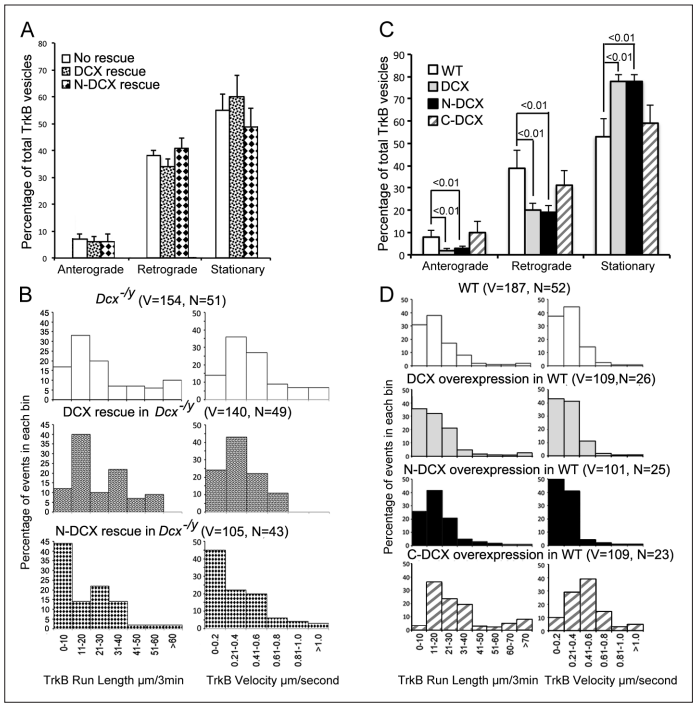

Figure 2—figure supplement 2. Doublecortin (DCX) affects the retrograde transport through DCX/dynein interaction. (**A**) Distribution calculations of the TrkB vesicle mobility status (anterograde, retrograde, and stationary) are demonstrated. No significant differences are observed among different neurons. (**B**) Run length and velocity distributions of retrograde TrkB complexes in axons from different neurons are shown. Total numbers of neurons (N) and vesicles (V) used in the calculations are indicated in the panel. (**C**) Distribution calculations of the TrkB vesicle mobility status (anterograde, retrograde, and stationary) in axons from WT cells with different transfections are demonstrated. Overexpression of DCX or N-DCX significantly increased percentage of stationary TrkB vesicles in axons, while decreased the percentile of both anterograde and retrograde transport. (**D**) Run length and velocity distributions of retrograde TrkB complexes in axons from different neurons are shown. Total numbers of neurons (N) and vesicles (V) used in the calculations are indicated in the panel.

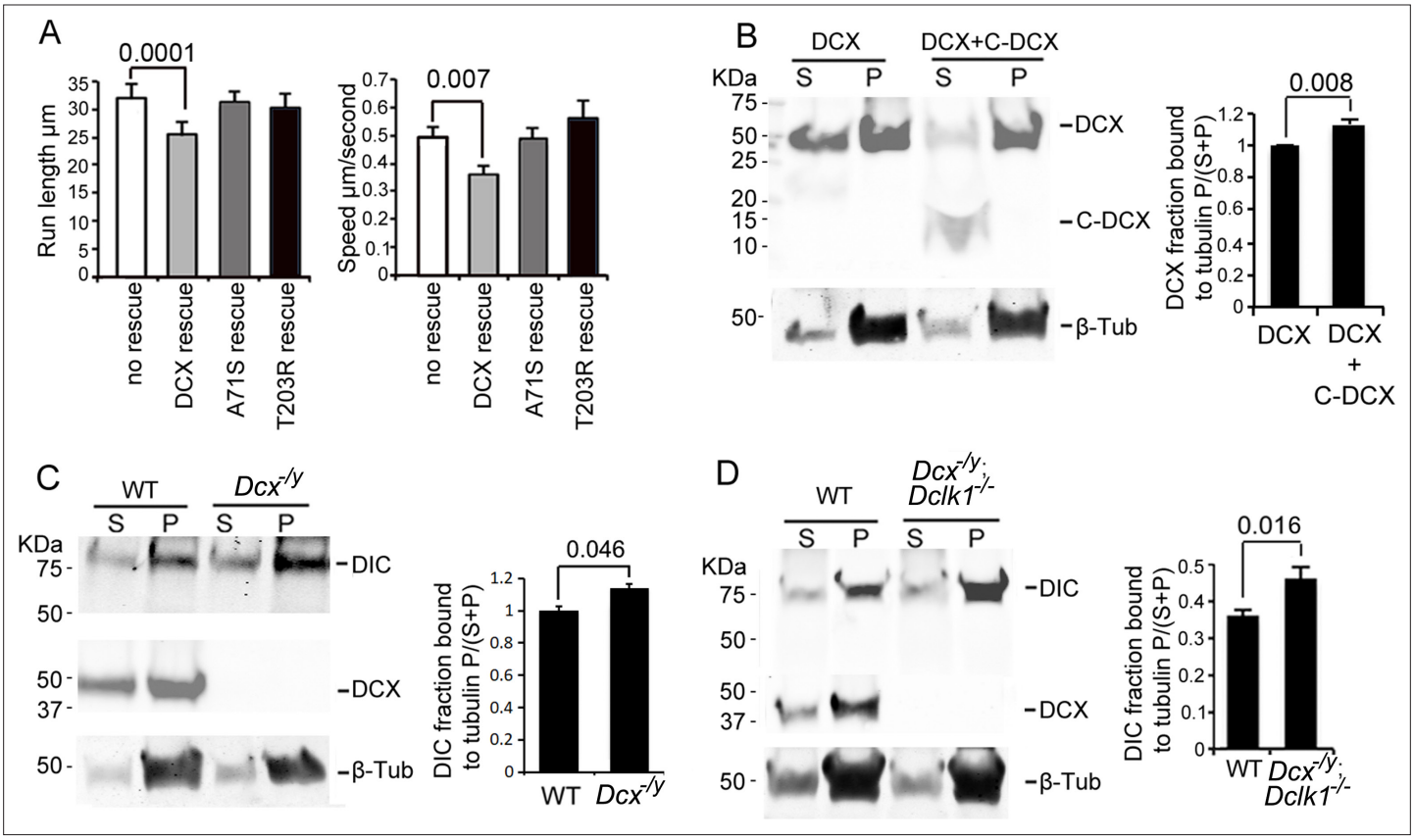

Figure 3. Doublecortin (DCX) association with microtubules (MTs). (**A**). Dissociated cortical neuronal cultures from WT or *Dcx*$^{-/y}$ mice were transfected with plasmids expressing TrkB-RFP with/without plasmids expressing DCX-GFP, DCXA71S, or DCXT203R on days in vitro (DIV)6 and imaged on DIV8. Quantification of Run length (mean +/- SEM) within 180 s and velocity (mean+/-SEM) is demonstrated. DCX, but not DCXA71S or DCXT203R, rescued the increased TrkB-RFP transport in DCX-deficient axons. All quantifications are based on three independent experiments of each condition. p-Values from *t*-tests are shown in each panel. Total numbers of neurons (N) and vesicles (V) used in the calculations are indicated in ***Figure 3—figure supplement 1***. (**B**). Protein lysate from HEK293 cells expressing HA-DCX or HA-DCX plus HA-C-DCX are incubated with exogenously added MTs, which are then pelleted by ultracentrifugation. Western blot for HA in supernatant (S) or pellet (P) is performed to determine the amount of DCX or C-DCX associated with MTs. Representative Western blots are shown. Fraction of DCX bound to tubulin is calculated (tubulin bound = P/(S + P)) and compared. Significantly more DCX is bound to MTs in the presence of C-DCX. p-Value from *t*-test is shown. (**C, D**) Brain lysate from P0 WT, *Dcx*$^{-/y}$ or *Dcx*$^{-/y}$;*Dclk1*$^{-/-}$ mice are incubated with exogenously added MTs, which are then pelleted by ultracentrifugation. Polymerized MTs are in the pellet. Western blot of dynein intermediate chain (DIC) in supernatant (S) or pellet (P) is performed to determine the amount of DIC associated with MTs. Representative Western blots are shown. Fraction of DIC bound to tubulin is calculated (tubulin bound = P/(S + P)) and compared between WT and *Dcx*$^{-/y}$; or WT and *Dcx*$^{-/y}$;*Dclk1*$^{-/-}$. Significantly more DIC is bound to MTs in the absence of DCX. p-Value from *t*-test is shown. All quantifications are based on three independent experiments.

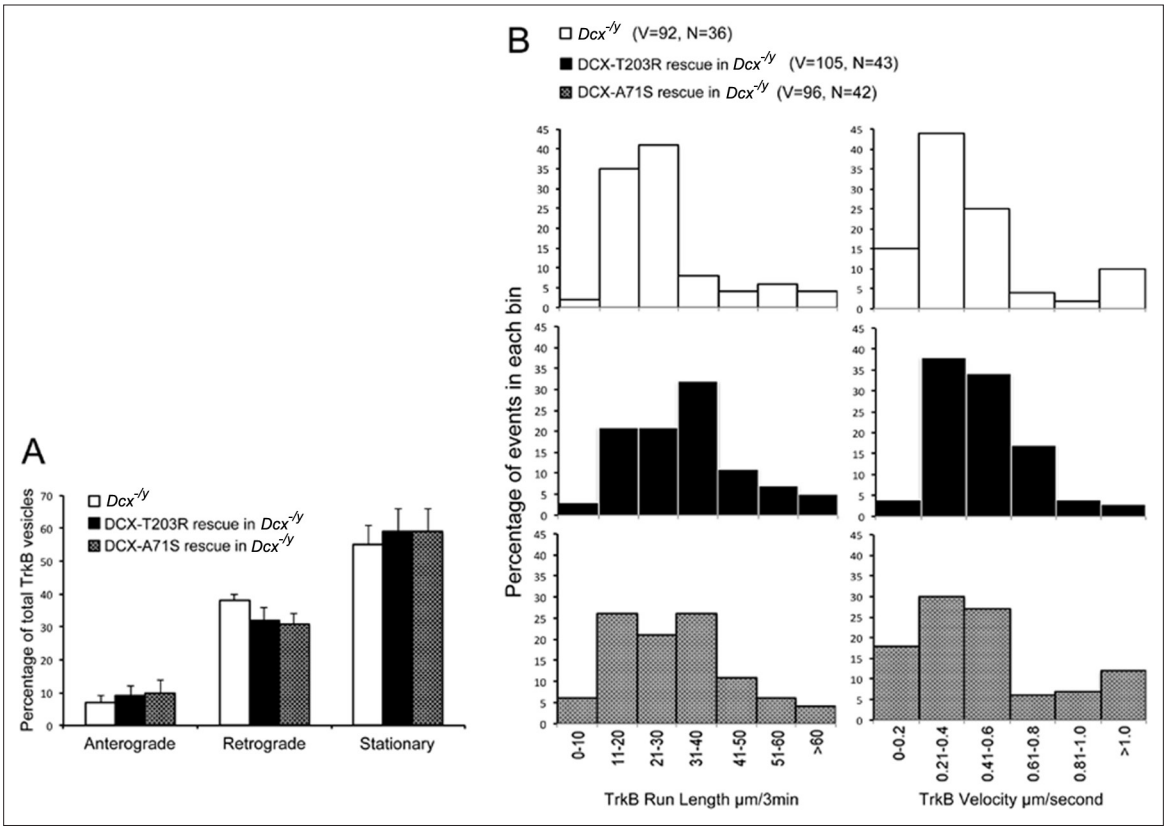

Figure 3—figure supplement 1. Doublecortin (DCX) effect on the retrograde trafficking needs DCX/microtubule (MT) interaction. (**A**) Distribution calculations of the TrkB vesicle mobility status (anterograde, retrograde, and stationary) in different cells are demonstrated. No significant differences are observed among different neurons. (**B**) Run length and velocity distributions of retrograde TrkB complexes in axons from different neurons are shown. Total numbers of neurons (N) and vesicles (V) used in the calculations are indicated in the panel.

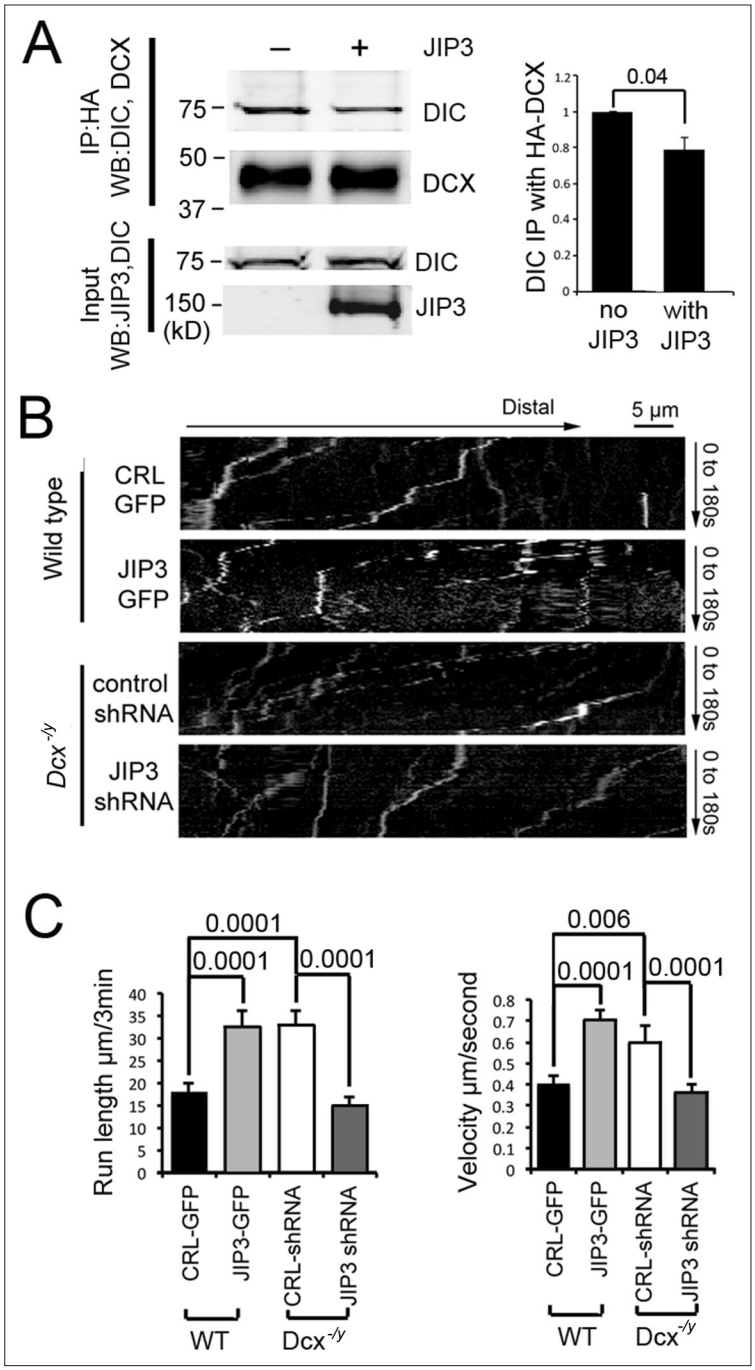

Figure 4. Doublecortin (DCX) and JIP3 competitively bind to the dynein motor complex, and JIP3 enhances retrograde transport mediated by dynein. (**A**) The presence of JIP3 decreases the interaction between DCX and dynein intermediate chain (DIC). HEK293 cells were transfected with plasmids expressing neuron-specific dynein intermediate chain isoform IC-1B and HA-tagged DCX with or without JIP3. Antibody for HA was used to precipitate HA-DCX and associated proteins. Western blot analysis of DIC and HA was performed to detect DIC immunoprecipitated with DCX. In the presence of JIP3, less DIC was associated with DCX, while total protein amount of either HA-DCX or DIC in the lysate was the same. Quantification of DIC bands of Western blot results (three independent experiments) after IP with HA were calculated and normalized with DIC levels in the lysate. p-Value from *t*-test is shown. (**B**) Cultured cortical neurons from P0 WT mouse brains were transfected with plasmids expressing TrkB-RFP with or without JIP3-GFP. Neurons from *Dcx*$^{-/y}$ mouse brains were transfected with plasmids expressing TrkB-RFP with or without JIP3 shRNA. Representative kymographs of TrkB-RFP trafficking are demonstrated. (**C**) Quantification of TrkB run length and velocity. Overexpression of JIP3 significantly increases

Figure 4 continued on next page

Figure 4 continued

run length and velocity of TrkB in WT neurons. Downregulation of JIP3 by shRNA in *Dcx*$^{-/y}$ neurons decreases TrkB retrograde transport. p-Values from *t*-tests are shown. All quantification data are based on three independent experiments of each condition. p-Values from *t*-tests are shown in each panel. Total numbers of neurons (N) and vesicles (V) used in the calculations are indicated in ***Figure 4—figure supplement 1***. See also ***Figure 4—video 1*** and ***Figure 4—video 2***.

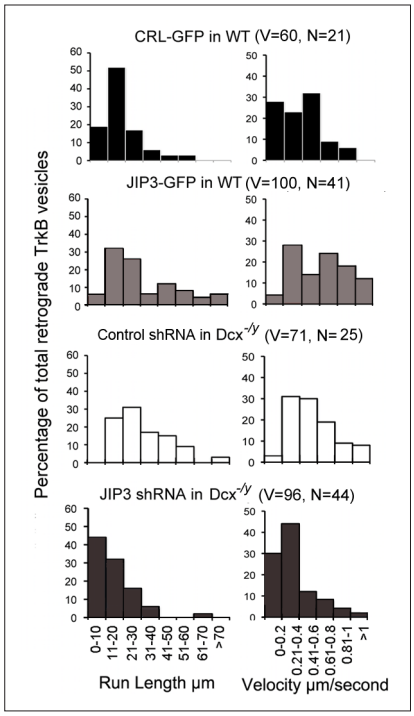

Figure 4—figure supplement 1. JIP3 enhances retrograde transport of TrkB. Run length and velocity distributions of retrograde TrkB complexes in axons from different neurons are shown.

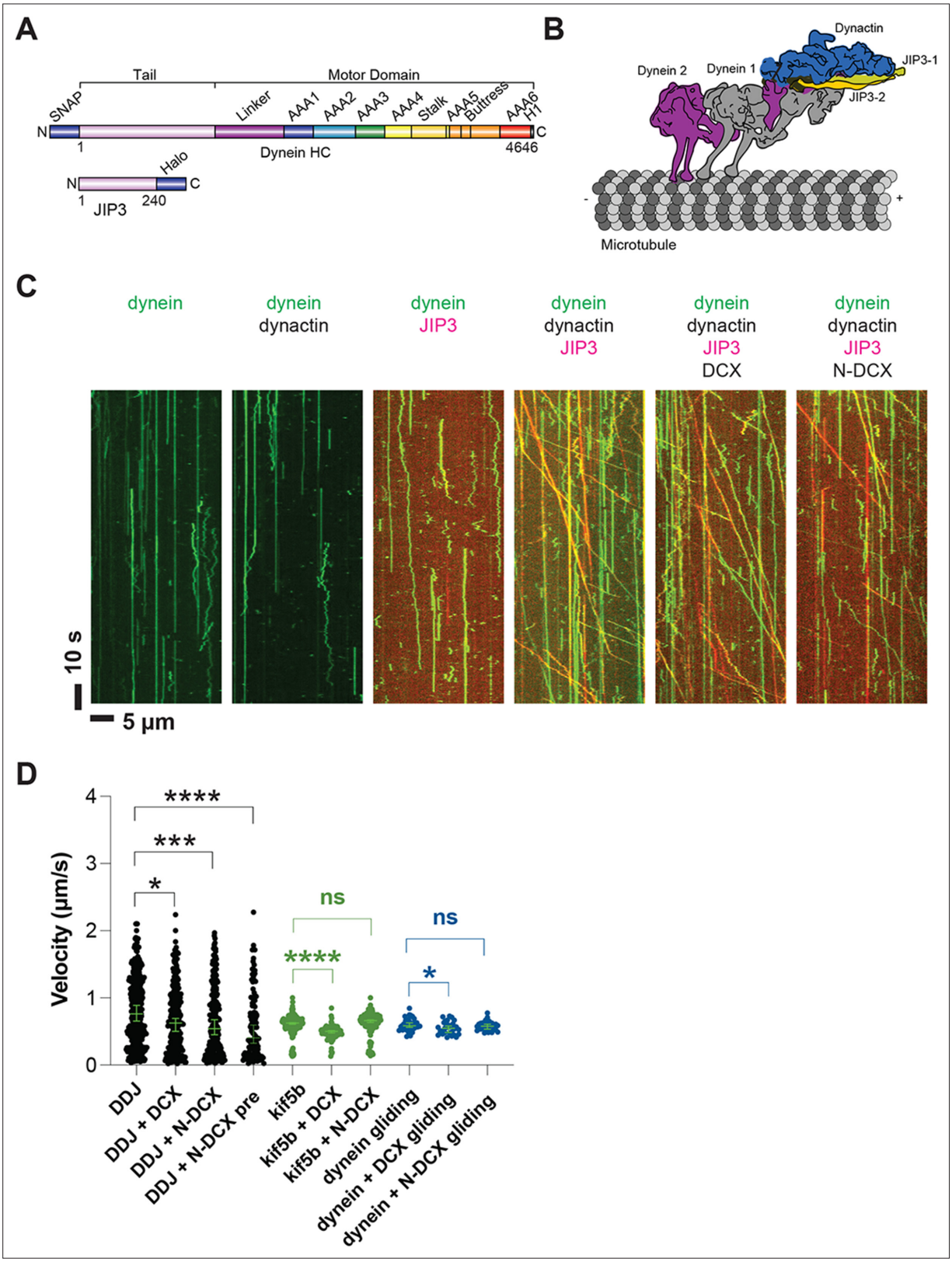

Figure 5. Dynein and dynactin form an active motor complex with JIP3 in vitro, and doublecortin (DCX) reduces its velocity. (**A**) Illustrations of the JIP3 and DCX constructs (left) and the DDJ motor complex (right). (**B**) Kymographs of dynein in the absence and presence of dynactin, JIP3, DCX, and N-DCX. Dynein was labeled with SNAP-TMR (green) and JIP3 was labeled with Halo-JP646 (red). (**C**) The velocity of DDJ motor complexes, KIF5B, and gliding MTs powered by surface-absorbed single-headed dynein. The green bars represent the median with 95% CI. DDJ (DDJ only): 0.76 [0.65, 0.89]

Figure 5 continued on next page

Figure 5 continued

μm/s; DDJ + DCX (DDJ with 10 nM DCX): 0.62 [0.50, 0.70] μm/s (KS test, *p<0.1); DDJ + N-DCX (DDJ with 10 nM N-DCX): 0.54 [0.45, 0.67] μm/s (KS test, ***p<0.001); DDJ + N-DCX pre (dynein, dynactin, JIP3, and N-DCX assembled in the ratio of 1:1:1:1): 0.41 [0.32, 0.60] μm/s (KS test, ****p<0.0001). kif5b (kif5b only): 0.63 [0.61, 0.63] μm/s; kif5b + DCX (kif5b with 10 nM DCX): 0.50 [0.48, 0.51] μm/s (unpaired *t*-test, ****p<0.0001); kif5b + N-DCX (kif5b with 10 nM N-DCX): 0.66 [0.64, 0.67] μm/s (unpaired *t*-test, n.s.). MT gliding (powered by single-headed human dynein): 0.59 [0.56, 0.63] μm/s; dynein + DCX (MT gliding with 10 nM DCX): 0.55 [0.48, 0.58] μm/s (unpaired *t*-test, *p<0.1); dynein + N-DCX (MT gliding with 10 nM N-DCX): 0.58 [0.53, 0.61] μm/s (unpaired *t*-test, n.s.). From left to right, n = 342, 275, 252, 115, 234, 103, 117, 33, 31, and 28. See also ***Figure 5—figure supplements 1–5*** and ***Figure 5—video 1***.

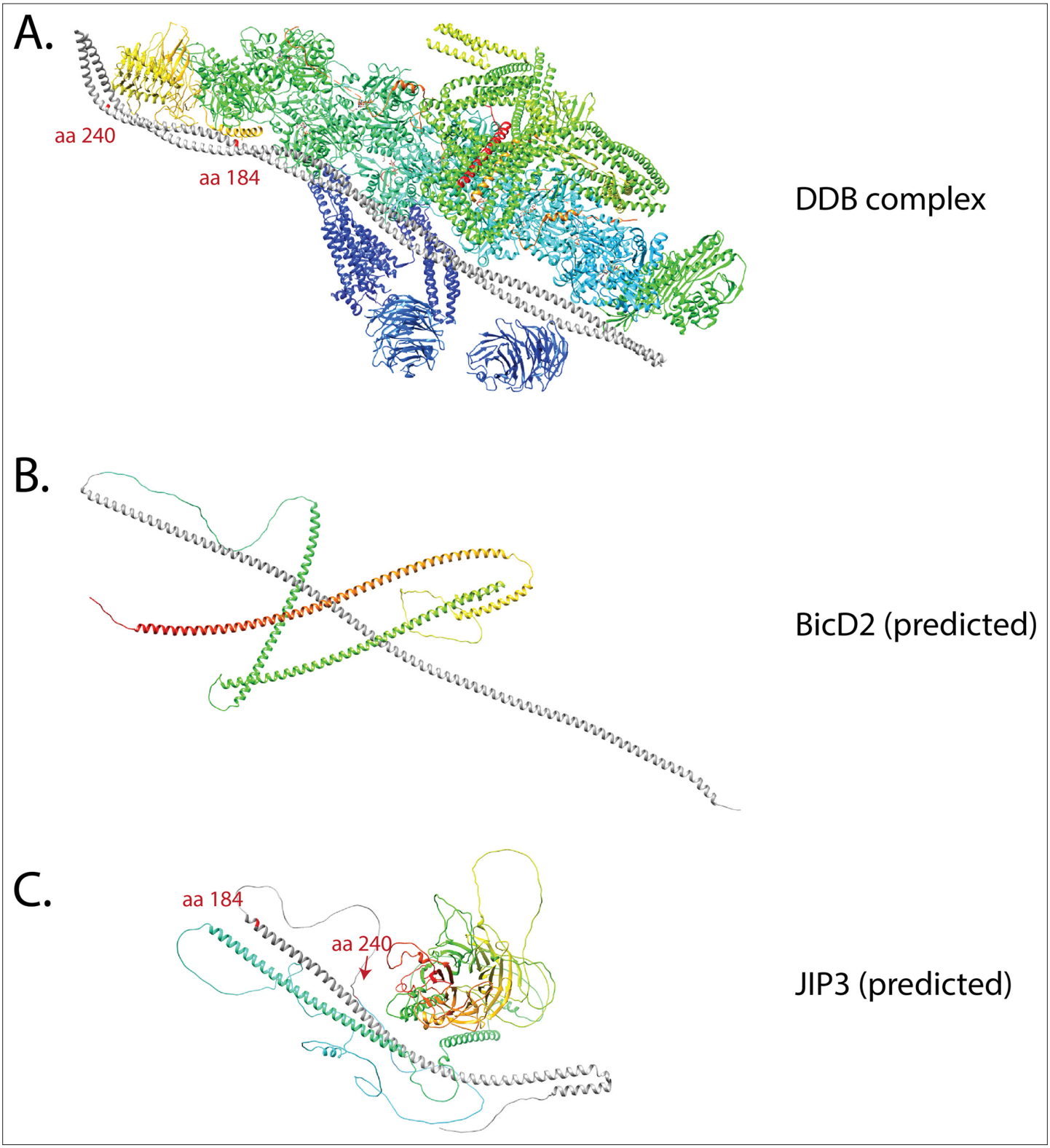

Figure 5—figure supplement 1. Comparison of the predicted structures of BicD2 and JIP3 with cryo-EM structure of DDB containing BicD2. (**A**) Cryo-EM structure of DDB complex (PDB 5AFU) (***Urnavicius et al., 2015***). The structure shows that the first coiled coil of BicD2 (dark gray) is up to aa 275, which spans the full length of dynactin shoulder. (**B**) Predicted BicD2 (UniProt Q8TD16) structure. The dark gray indicated the first α-helix that was predicted to extend to aa 272 (***Jumper et al., 2021***), which corresponds to the cryo-EM structure. (**C**) Predicted JIP3 (UniProt Q9UPT6) structure. The dark gray indicated the first α-helix is predicted to be up to aa184. The region between aa 185 and aa 240 was predicted to be disordered. The red

Figure 5—figure supplement 1 continued on next page

Figure 5—figure supplement 1 continued

labels in (**A**) indicate the beginning (aa 6) of the BicD2 α-helix, the position of aa 187 to show the estimated end of the predicted α-helix in JIP3 in (**C**), and the position of aa 240 to show the estimated aa 240 position of JIP3, should the disorder region of JIP3 forms α-helix upon interaction with dynactin. The red labels in (**B**) and (**C**) indicate the beginning and end of the predicted first α-helix in BicD2 and JIP3, respectively.

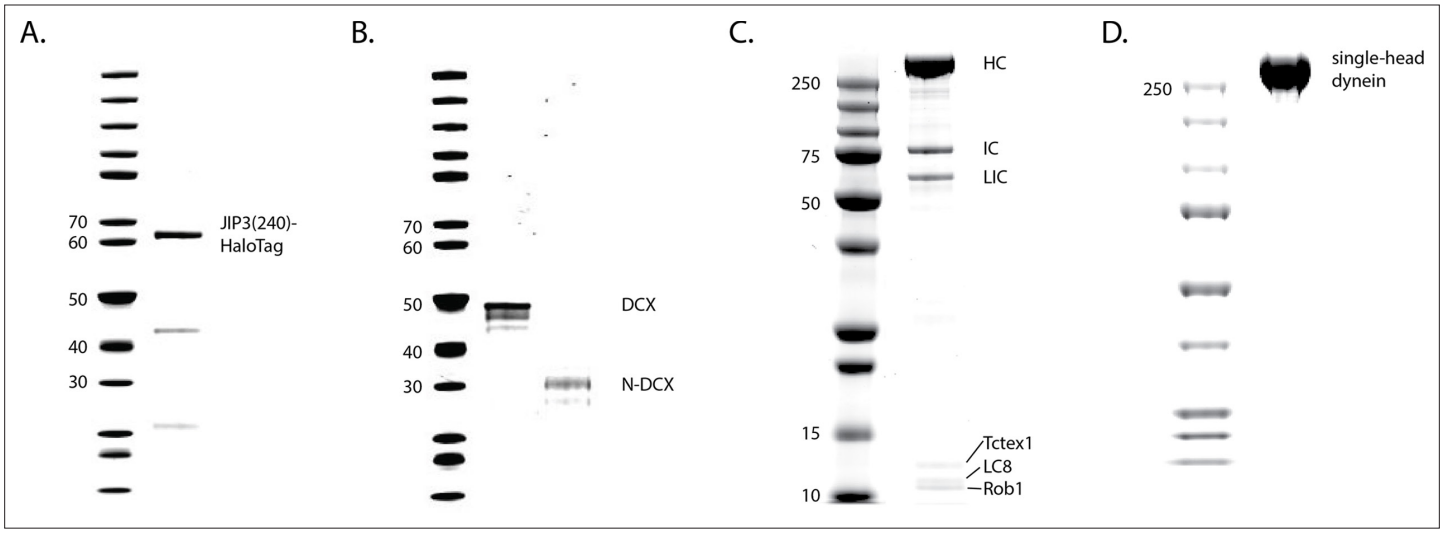

Figure 5—figure supplement 2. PAGE gels of recombinant expressed proteins. (**A**) JIP3(aa1-240)-HaloTag. (**B**) DCX-ybbR and N-DCX-ybbR. (**C**) Human dynein complex, containing a heavy chain (HC) with a SNAP-tag, an intermediate chain (IC), a light intermediate chain (LIC), and three light chains (Tctex1, LC8, Rob1). (**D**) Single-head human dynein-GFP.

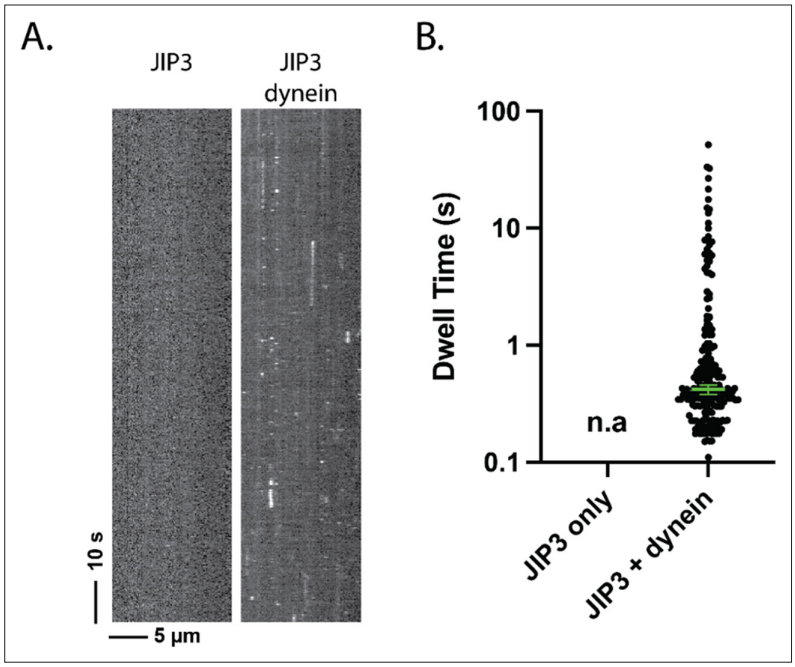

Figure 5—figure supplement 3. JIP3 has a transient affinity for dynein. (**A**) Kymograph of JIP3 on microtubules, without (left) or with (right) dynein present. Without dynein, JIP3 shows no affinity for microtubules; in the presence of dynein, JIP3 demonstrated brief binding events via dynein. The concentration of dynein was 1 nM, and the concentration of JIP3 was 10 nM. (**B**) The dwell time JIP3 on microtubule via dynein. Without dynein, there was no measurable dwelling of JIP3; with dynein, the dwell time of JIP3 on dynein is 0.42 [0.38, 0.46] s (median [95% CI]).

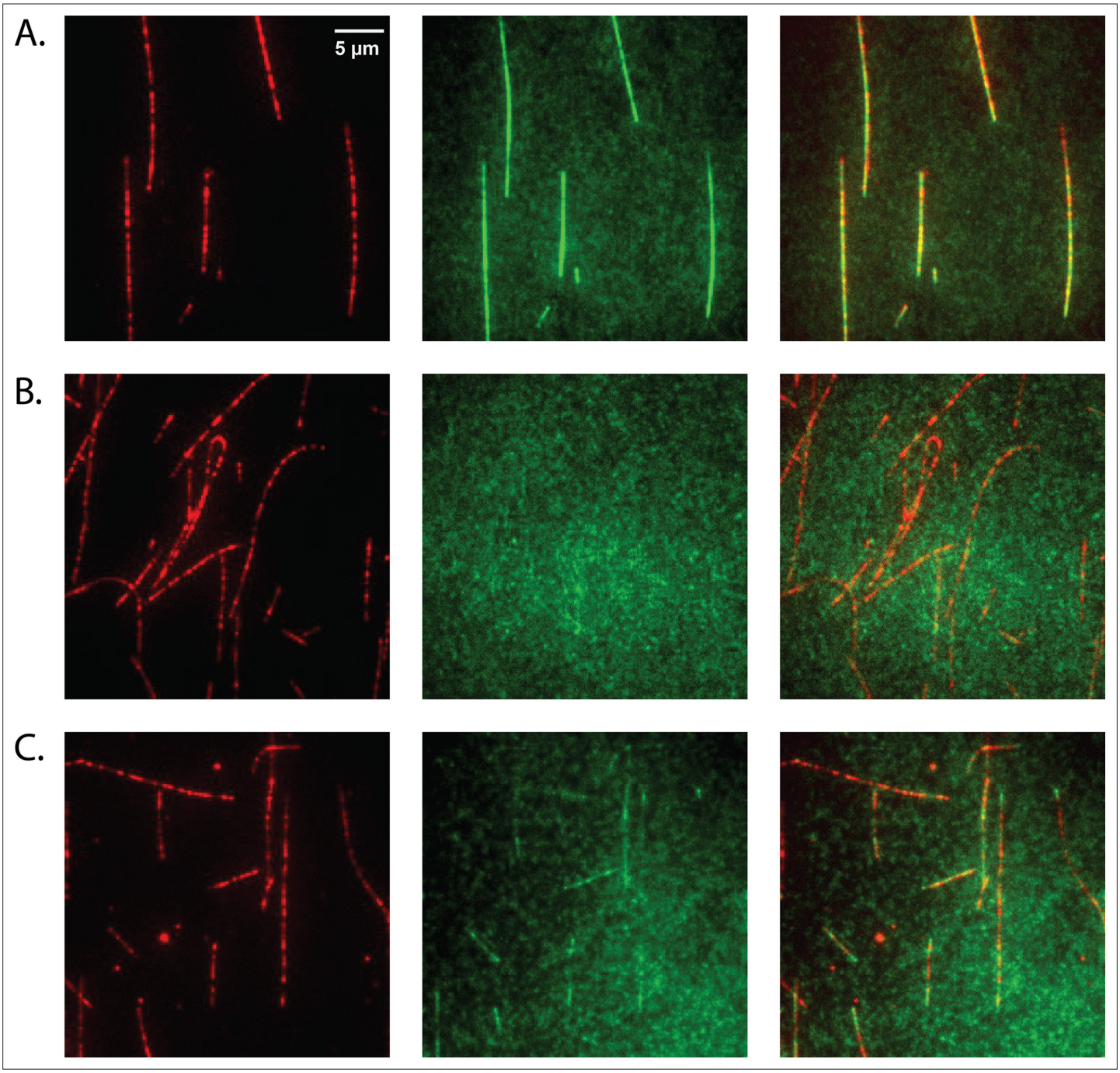

Figure 5—figure supplement 4. Doublecortin (DCX) binds microtubules (MTs). (**A**) At 10 nM concentration, DCX uniformly decorates MTs. DCX-ybbR was labeled with CoA-CF488, and MTs were labeled with Cy5. (**B**) At 10 nM concentration, N-DCX does not bind to MTs in the motility buffer. N-DCX-ybbR was labeled with CoA-CF488. (**C**) At 10 nM concentration, N-DCX decorates MTs in a buffer that is half of the ionic strength of motility buffer.

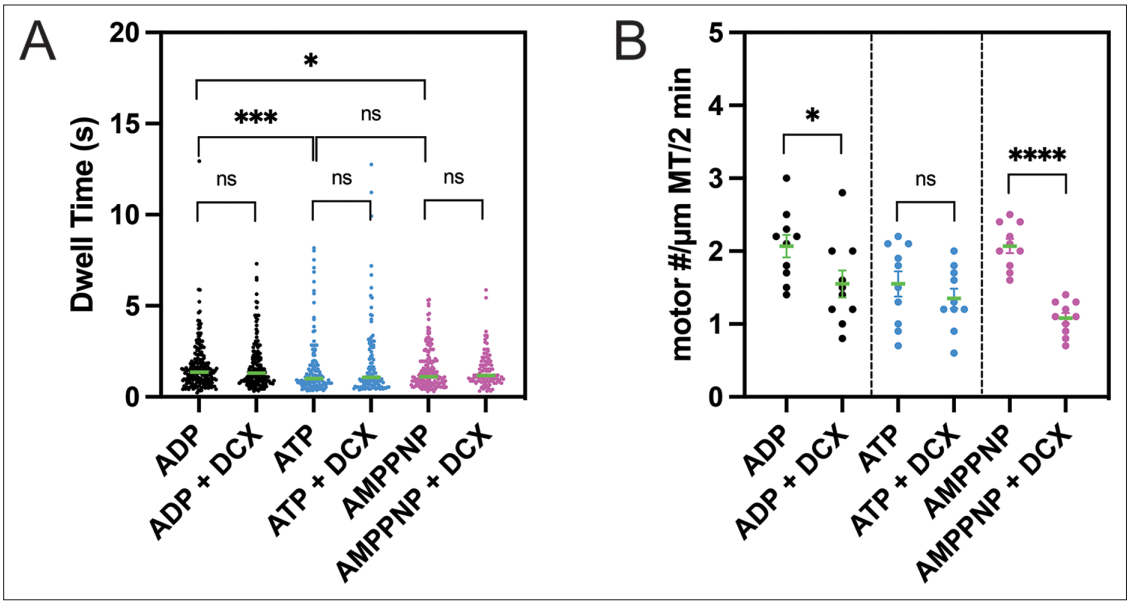

Figure 5—figure supplement 5. Doublecortin's (DCX's) effects on the microtubule (MT) on-rate and the MT-bound time of single-headed human dynein. (**A**) The dwell time of single-head human dynein on MTs in various nucleotide states is not altered by DCX. Unpaired Kolmogorov–Smirnov *t*-test was performed. ns (not significant), p>0.1; *p<0.1; ***p<0.001. The green bars represent the median values: ADP: 1.4 s (n = 206); ADP + DCX: 1.3 s (n = 187); ATP: 1 s (n = 140); ATP + DCX: 1.1 s (n = 120); AMPPNP: 1.1 s (n = 166); AMPPNP + DCX: 1.2 s (n = 111). (**B**) In AMPPNP and ADP state, the landing rate of single-head human dynein on MTs is reduced by DCX, while in ATP state, the rate is unaffected. For each condition, the numbers of motors on 10 MTs were counted. Unpaired *t*-test was performed. ns (not significant), p>0.1; *p<0.1; ****p<0.0001. The green bars represent the mean with SEM: ADP: 2.1 ± 0.2; ADP + DCX: 1.6 ± 0.2; ATP: 1.6 ± 0.2; ATP + DCX: 1.4 ± 0.1; AMPPNP: 2.1 ± 0.1; AMPPNP + DCX: 1.1 ± 0.1.

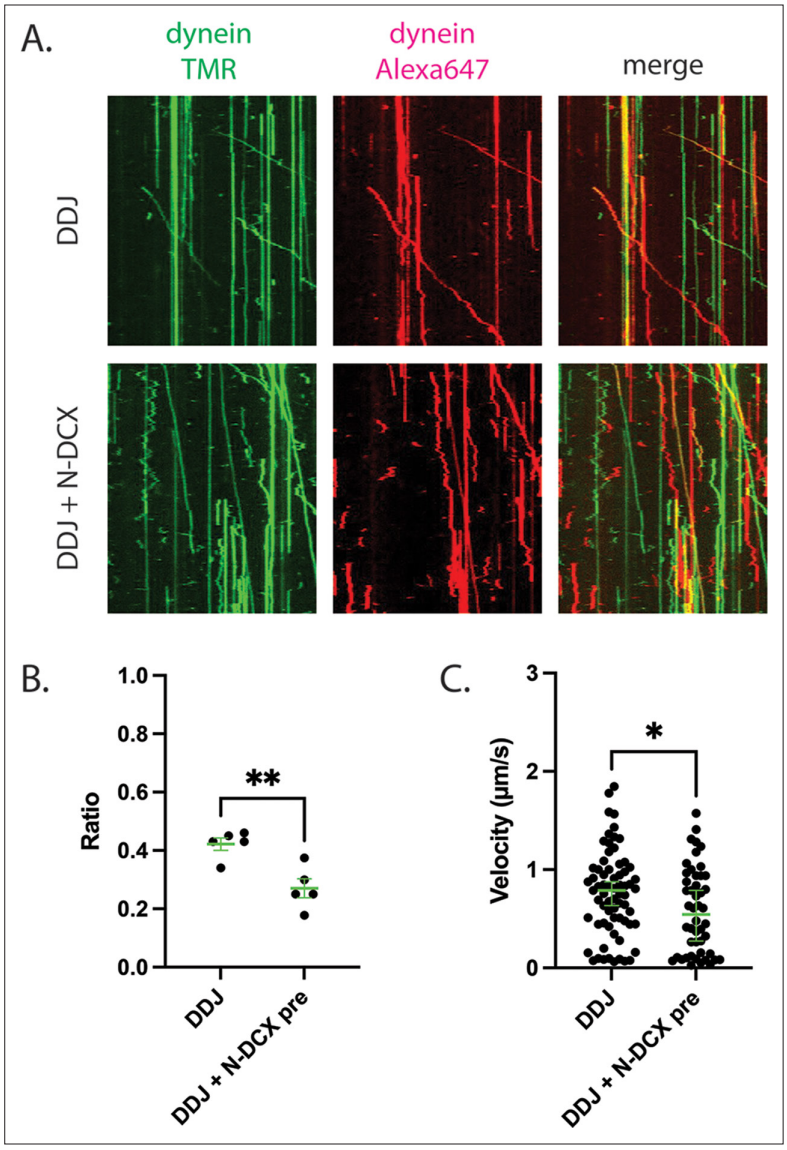

Figure 6. DDJ motor complexes associate with two dyneins, and N-DCX negatively affects its velocity by displacing the second dynein. (**A**) Kymograph of DDJ assembled in the absence (top) or presence (bottom) of N-DCX with dynein that were labeled separately with SNAP-TMR and SNAP-Alexa 647. (**B**) The ratio of two-color moving molecules versus the total moving molecules. The green bars represent mean ± SEM. DDJ: 42 ± 2%; DDJ + N-DCX pre: 27 ± 3% (unpaired *t*-test, **p<0.01). The molecules within each field of view were counted to produce a single value (50 µm × 50 µm). (**C**) The velocity of two-color moving molecules. The green bars represent median with 95% CI. DDJ: 0.79 [0.63, 0.87] µm/s; DDJ + N-DCX pre: 0.54 [0.27, 0.79] µm/s (KS test, *p<0.1).

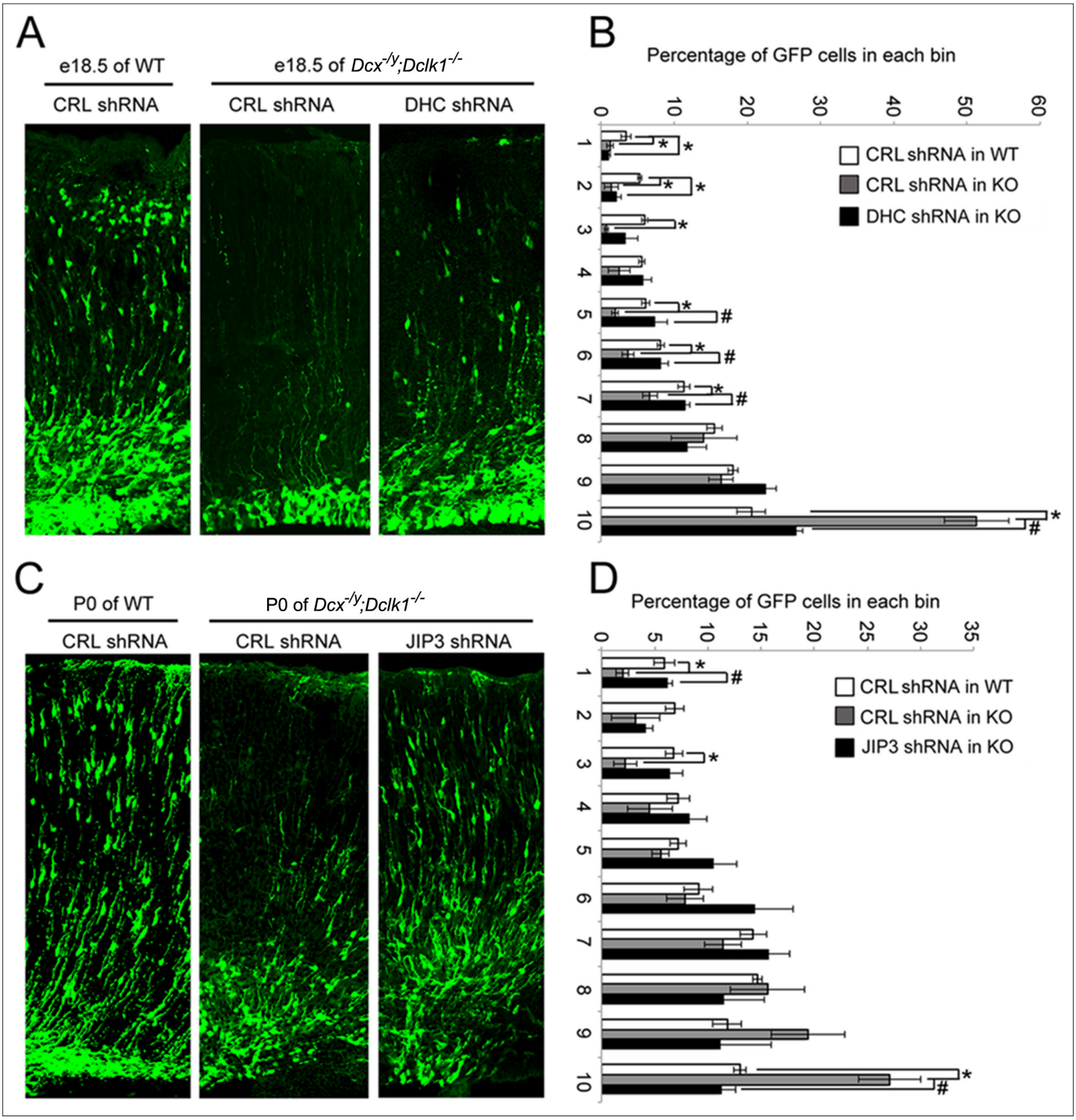

Figure 7. Knockdown of DHC or JIP3 in *Dcx*$^{-/y}$;*Dclk1*$^{-/-}$ in mouse cortex partially rescues the defect of pyramidal cell migration. (**A**) GFP-positive neurons were imaged and counted at embryonic day (E)18.5 after electroporation at E14.5 with vectors expressing control (CRL) shRNA (+GFP) or DHC shRNA (+GFP). (**B**) Percent of GFP-positive cells in evenly divided regions of the cortex (1–10) from the pia to the lateral ventricle. Asterisks denote statistically significant p-values (*t*-test, p<0.05) between WT with CRL shRNA and *Dc*$^{x-/y}$;*Dclk1*$^{-/-}$ with CRL shRNA. Number sign (#) denotes p<0.05 of *t*-test between *Dcx*$^{-/y}$;*Dclk1*$^{-/-}$ with CRL shRNA and *Dcx*$^{-/y}$;*Dclk1*$^{-/-}$ with DHC shRNA. The data represent the mean ± SEM of three different brains in each condition. (**C**) GFP-positive neurons were imaged and counted at P0 after electroporation at E14.5 with vectors expressing control (CRL) shRNA (+GFP) or JIP3 shRNA (+GFP). (**D**) Percent of GFP-positive cells in evenly divided regions of the cortex (1–10) from the pia to the lateral ventricle of different mouse brains. * denotes p<0.05 of *t*-test between WT with CRL shRNA and *Dcx*$^{-/y}$;*Dclk1*$^{-/-}$ with CRL shRNA. Number sign (#) denotes p<0.05 of *t*-test between *Dcx*$^{-/y}$;*Dclk1*$^{-/-}$ with CRL shRNA and *Dcx*$^{-/y}$;*Dclk1*$^{-/-}$ with JIP3 shRNA. The data represent the mean ± SEM of three individual brains in each condition.

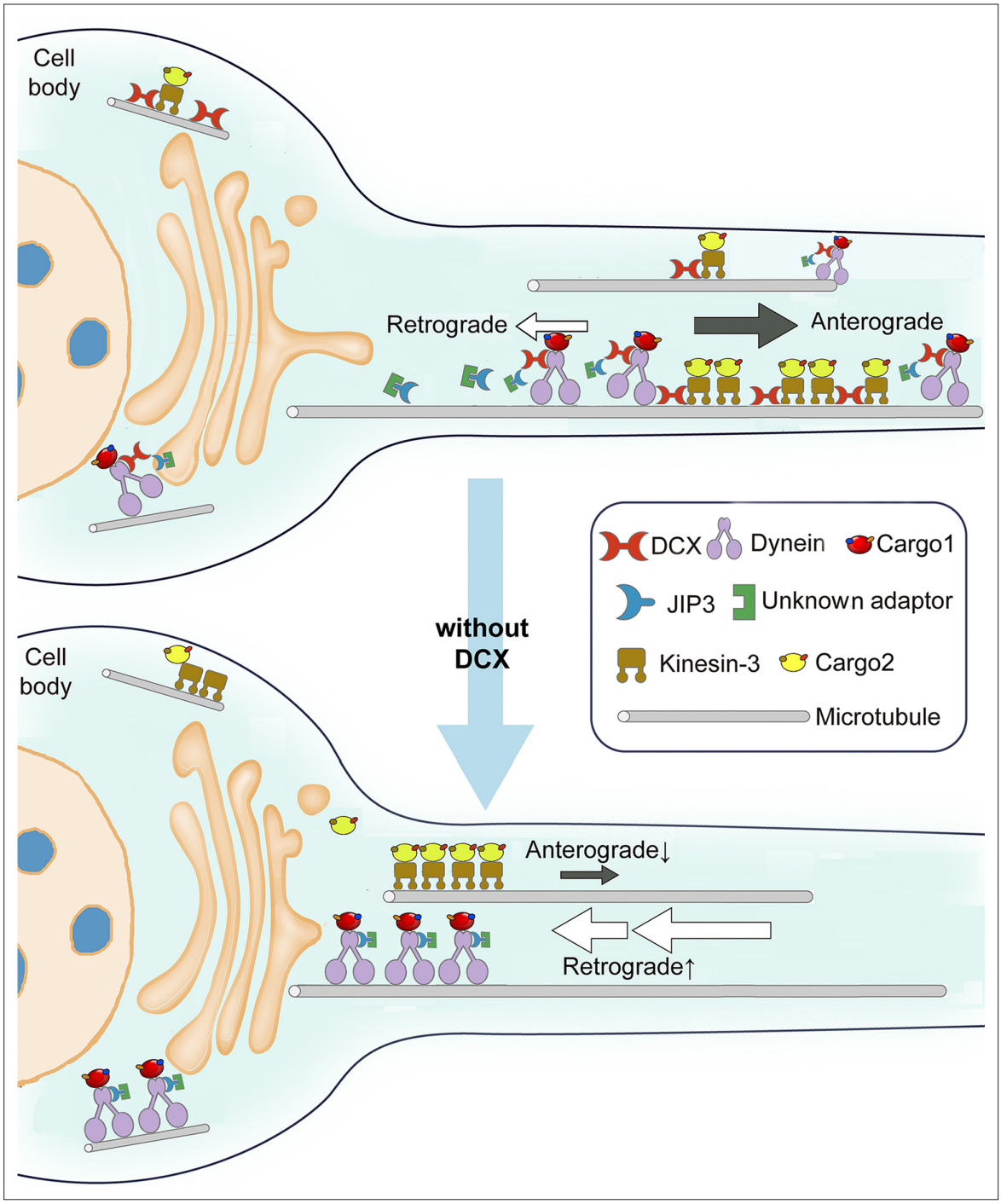

Figure 8. Schematic diagram shows the regulation of dynein-mediated retrograde transport by doublecortin (DCX). Cargo-bound dynein motor complex drives retrograde transport from plus end of microtubules (MTs) (distal axon) to minus end of MTs (cell body). In WT neurons, DCX association with kinesin-3 helps kinesin-3-mediated anterograde transports (***Liu et al., 2012***). DCX decreases dynein-MT interactions (represented by tilted dynein complex along MT). DCX and JIP3 competitively associate with dynein. When DCX binds dynein, very few JIP3 proteins associate with dynein, the retrograde transport is normal. In DCX KO neurons (without DCX), kinesin-3-mediated anterograde transports are decreased without DCX (***Liu et al., 2012***). Meanwhile, more JIP3 molecules bind dynein, which also associates with MT stronger without DCX. The dynein-mediated retrograde transport is faster. The balance between anterograde transport and retrograde transport is broken without DCX.